Surface Raman scattering and electrochemistry of iron protoporphyrin IX at a polycrystalline silver electrode

J. J. McMahon, S. Baer, and C. A. Melendres

J. Phys. Chem., **1986**, 90 (8), 1572-1577 • DOI: 10.1021/j100399a023

Surface Raman Scattering and Electrochemistry of Iron Protoporphyrin IX at a Polycrystalline Silver Electrode

J. J. McMahon,*† S. Baer, and C. A. Melendres

Thompson Chemical Laboratory, Williams College, Williamstown, Massachusetts 01267, and Chemical Technology Division/Materials Science and Technology Division, Argonne National Laboratory, Argonne, Illinois 60439 *(Received: October 14, 1985)*

Cyclic voltammetry and laser Raman spectroscopy were used to characterize in situ the behavior of iron(III) protoporphyrin IX (Fe(III)PP) adsorbed at a polycrystalline silver electrode in 0.1 M $Na_2B_4O_7$ electrolyte solution. Modest catalysis of the O_2 reduction reaction in the presence of porphyrin was observed. Reduction of the Fe(III)PP to Fe(II)PP in solution was distinguishable from that of adsorbed hemin. Solution electrochemistry and resonance Raman scattering following reduction suggest that, while dimerization of the reduction product appears to occur in solution, the surface bound species remain monomeric.

Introduction

Considerable work is being done on transition-metal macrocyclic compounds, e.g., metal porphyrins and phthalocyanines, not only because of their biological significance,[1] but also because of their potential practical application in electrochemical energy storage and conversion devices.[2] Significant progress has been made in understanding the physicochemical properties and chemistry of these materials. Many questions regarding their role in facilitating oxygen transport and reduction, however, still remain unanswered. Our interest in macrocyclic compounds lies in their possible use to substitute for precious metals (e.g., Pt) as oxygen reduction catalysts in batteries and fuel cell systems. Iron and cobalt phthalocyanine, for example, appear to have activities nearly equal to that of platinum although their stability is still not sufficient for commercial use.[3,4] We believe that a thorough understanding of the structure and properties of these compounds would be the key to improving their stability and/or leading the way toward the synthesis of better catalysts. We are, therefore, conducting electrochemical and spectroscopic investigations in order to obtain correlation between the structure and interfacial properties of these and similar materials. In the present communication, we report results of our initial studies on iron protoporphyrin IX (FePP). We show the value of coupled spectro-electrochemical techniques in elucidating processes occurring at the electrode–solution interface.

Experimental Section

The silver electrodes were prepared from 0.025-cm Ag foils (marz grade, 99.999% purity, obtained from Materials Research Corp., Orangeburg, NY). These were abraded with size 600 grit emery cloth before use. Iron(III) protoporphyrin IX chloride (FePPCl) was dissolved in 0.1 M sodium borate ($Na_2B_4O_7$, pH 9.3) supporting electrolyte. In dilute solutions of FePPCl, KCl was added (0.1 M) to facilitate anodization of Ag to AgCl. Similar results were obtained in solutions of dilute base (NaOH) at an equivalent pH. Electrochemical and in situ laser Raman spectroscopic measurements were performed in solutions ranging from 10^{-7} to 10^{-3} M hemin concentration. Adsorption of FePP on silver usually occurred in situ upon electrode immersion and was further effected by anodization followed by a sweep to cathodic potentials. For ex situ laser Raman spectroscopic studies, FePP was adsorbed on Ag by dipping the silver electrode into either (i) a solution of 0.25 wt % FePPCl in pyridine or (ii) 10^{-3} M FePPCl in 0.1 M $Na_2B_4O_7$. The electrochemical cell used for in situ laser Raman spectroscopy measurements was previously described.[4] Electrode potentials were controlled by either an Eco Instruments Model 149 potentiostat which was modulated by an interfaced Apple II+ microcomputer or a PAR Model 173 potentiostat and Model 179 universal programmer. Reproducible charge development during the anodization cycle was effected with an Eco Instruments Model 731 current integrator interfaced with the Apple. All potentials reported here are referenced with respect to the saturated calomel electrode (SCE). Spectra were obtained with a Spex Model 1403 double monochromator with a photomultiplier tube detector operated in the photon counting mode. Laser excitation was provided by Coherent Radiation Model CR6 Ar^+ and Model 750 K Kr^+ lasers. Spectra were taken using excitations at 4880 Å (Ar^+), 4579 Å (Ar^+), 5145 Å (Ar^+), 6471 Å (Kr^+), and 4067 Å (Kr^+).

Results and Discussion

Electrochemical Measurements. Figure 1 illustrates typical cyclic voltammograms at a silver electrode in 0.1 M sodium borate electrolyte at ambient with (broken lines) and without (solid lines) FePPCl (10^{-3} M). Both scans were initiated with a sweep from 0.1 V (with an open circuit voltage at 0.144 V) and scanned toward anodic potentials at a sweep rate of 20 mV/s.

In the absence of added FePPCl, anodic current is first observed during the electrodissolution of silver to Ag^+ (wave I_a) with subsequent chemical reaction to form what we believe to be AgH_2BO_3 ($B_4O_7^{2-}$ disproportionates to $H_2BO_3^-$ and H_3BO_3 in alkaline solutions). During the subsequent cathodic sweep, redeposition of silver metal occurs as exhibited by a wave with a peak potential at 0.232 V (I_c). Reduction of dissolved oxygen appears next in the cathodic sweep with peak potential at −0.375 V (II_c). The latter wave was found to correspond to a diffusion-controlled process with the peak current showing linearity with the square root of the scan rate.

In solutions containing 10^{-3} MFePPCl the anodization of silver gives rise to a wave with a peak potential of 0.258 V (1_a); a corresponding reduction wave is observed at −0.059 V (1_c). We assign these waves to the formation of AgCl and its subsequent reduction. The chloride has its origin from the dissociation of FePPCl. In basic solutions, formation of the μ-oxo dimer[5] of FePP is known to occur. Oxygen reduction is followed by another process as evidenced by the excess cathodic current (2_c) over that observed in the solution without FePPCl. Anodic current (2_a) is also observed on the return sweep to 0.1 V.

Figure 2 compared more closely the reduction of oxygen on Ag and in the presence of FePP. As can be seen, a modest catalysis of the O_2 reduction is indicated by an anodic shift (~70 mV) of the peak potential of the wave in the presence of adsorbed FePP

† Thompson Chemical Laboratory.

(1) Falk, J. E. "Porphyrins and Metalloporphyrins"; Elsevier: New York, 1964.
(2) Jahnke, H.; Schonborn, M.; Zimmerman, G. *Top. Curr. Chem.* **1976**, *61*, 133.
(3) Van Veen, J. A. R.; van Baer, J. F. *Ber. Bunsenges. Phys. Chem.* **1981**, *85*, 693.
(4) Melendres, C. A.; Cafasso, F. A. *J. Electrochem. Soc.* **1981**, *128*, 755.
(5) Cohen, I. A. *J. Am. Chem. Soc.* **1969**, *91*, 1980; Smith, K. M., Ed. "Porphyrins and Metalloporphyrins"; Elsevier: New York, 1973.

0022-3654/86/2090-1572$01.50/0

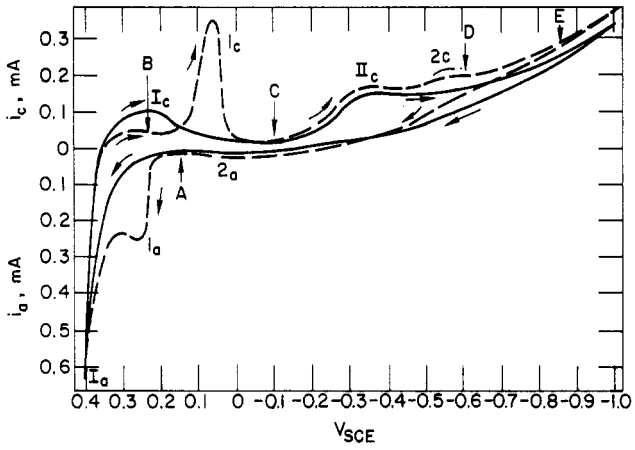

Figure 1. Cyclic voltammograms for $Ag/Na_2B_4O_7$ and $Ag/Na_2B_4O_7$, FePPCl solutions: —, 0.1 M $Na_2B_4O_7$, air saturated; ----, 0.1 M $Na_2B_4O_7$, 0.001 M FePPCl, air saturated; electrode area ~ 1 cm^2; scan rate = 20 mV/s.

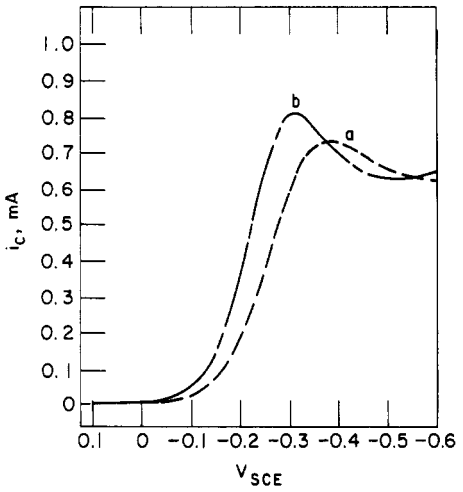

Figure 2. O_2 reduction on Ag with (a) and without (b) FePPCl; (a) 0.1 M $Na_2B_4O_7$, 0.001 M FePPCl, O_2 saturated solution; (b) 0.1 M $Na_2B_4O_7$, O_2 saturated; electrode area ~ 1 cm^2; scan rate = 20 mV/s.

(curve b) as compared to that on pure silver (curve a).

The faradaic electrode processes involving the FePP may be examined more thoroughly in solutions where oxygen has been excluded. Dissolved oxygen was removed by passing purified helium (99.99%) over copper turnings heated to 550 °C and bubbling the effluent through all three electrode chambers. The oxygen content was monitored by potentiostating at −0.3 V where the observed cathodic current was then allowed to reach a steady-state minimum prior to electrochemical and Raman studies.

Figure 3 shows typical cyclic voltammograms obtained from deoxygenated solutions of 15 μM FePPCl in 0.1 M KCl and dilute NaOH (pH 10.5). Similar voltammograms were obtained in 0.1 M sodium borate solution. Three cathodic waves I_c, II_c, and III_c were observed in the cathodic sweep to −1.2 V. Jordan and Bednarski[6] identified wave II_c as a two-electron reduction of a hemin dimer, probably the μ-oxo bridged dimer,[5] resulting in the formation of monomers. The main wave and the barely visible prewave were also observed by Davis and Martin.[7] They observed prewave I_c to be independent of hemin concentration and directly proportional to the surface area of a mercury electrode as is characteristic of electrolysis of adsorbed species. As will be seen subsequently in the next section, the potential dependence of the surface Raman scattering for adsorbed FePP supports this assignment of wave I_c to the reduction of adsorbed hemin.

Though wave I_c has been correlated with reduction of adsorbed hemin, wave II_c cannot be assigned to reduction of strictly dissolved

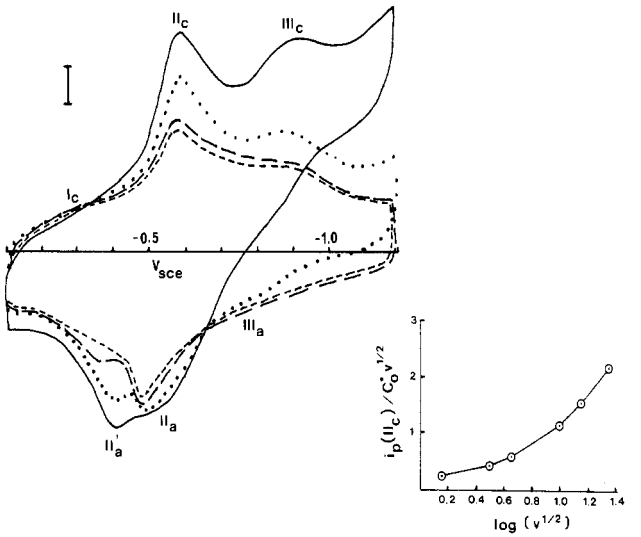

Figure 3. Scan rate dependence of cyclic voltammetry for 15 μM FePPCl in 0.1 M KCl and dilute NaOH (pH 10.5): —, 2 mV/s, 1-μA scale; ····, 10 mV s, 5-μA scale; – – –, 100 mV/s, 50-μA scale; ----, 200 mV/s, 100-μA scale.

TABLE I: Scan Rate Dependence of Wave II_a Relative to Wave II_a' in Figure 3

scan rate, mV/s	peak current, μA		ratio
	II_a	II_a'	$i_p(II_a)/i_p(II_a')$
2	3.4	4.78	0.712
10	21.5	20.75	1.036
100	207.5	152.5	1.360
200	202.5	135.0	1.500

hemin. Following the diagnostic criteria of Wopschall and Shain[8] we first note that, at the low concentration of 15 μM FePP, the symmetry of wave II_c indicated electrolysis of an adsorbed species rather than electrolysis of a diffusing reactant. Next, a plot of $i_p/C_0^* v^{1/2}$ as a function of log ($v^{1/2}$) is not constant (Figure 3) and is characteristic[9] of a weakly adsorbed reactant. Wave II_c, therefore, represents the reduction of both solution hemin and weakly adsorbed hemin.

Association of both waves I_c and II_c with reduction of adsorbed hemin suggests two different types of surface binding for the adsorbate. Since wave I_c is anodic of wave II_c, which has been linked to reduction of weakly adsorbed hemin, wave I_c can be assumed to represent reduction of more strongly bound hemin.

The anodic halves of waves II and III are observable on the return scan. The anodic complement to wave I_c is probably obscured by the less reversible main wave II_a. As observed in Figure 3, another wave, II_a', becomes visible on the anodic side of wave II_a at slow scan rates. We checked the dependence of wave II_a' on the solution concentration of reduced hemin, Fe(II)PP, by examining the scan rate dependence of the peak currents for waves II_a and II_a'. Table I reveals an increased ratio $i_p(II_a)/i_p(II_a')$ with increased scan rate; i.e., at lower scan rates, where the concentration of Fe(II)PP is higher, $i_p(II_a')$ is also higher. Association of wave II_a' with oxidation of adsorbed species, as suggested by Davis and Martin,[7] can be excluded because of the dependence of $i_p(II_a')$ on the solution concentration of reduced hemin. Furthermore, the appearance of wave II_a' only at elevated Fe(II)PP concentrations suggests the presence of Fe(II)PP dimers in solution. Apparently, some of Jordan and Bednarski's[6] product monomers aggregate when the solution concentration of Fe(II)PP is sufficiently high. This is not totally unexpected since Fe(II)PP is uncharged and would be expected to aggregate in aqueous solutions. The presence of Fe(II)PP dimers in solution is further suggested by observed differences in the resonance Raman scattering spectrum of the reduced solution compared to the

(6) Jordan, J.; Bednarsky, T. M. *J. Am. Chem. Soc.* **1964**, *86*, 5690.
(7) Davis, D. G.; Martin, R. F. *J. Am. Chem. Soc.* **1966**, *88*, 1365.
(8) Wopschall, R. H.; Shain, I. *Anal. Chem.* **1967**, *39*, 1514.
(9) Wopschall, R. H.; Shain, I. *Anal. Chem.* **1967**, *39*, 1535.

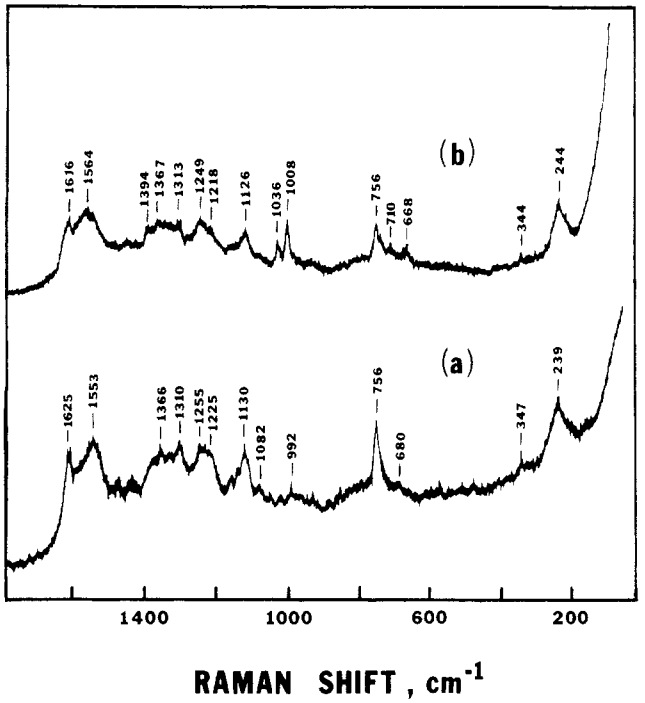

Figure 4. Ex situ surface Raman spectra of FePPCl on Ag: (a) electrode immersed in FePPCl-saturated, 0.1 M $Na_2B_4O_7$ solution; (b) electrode immersed in 0.30 wt. % FePPCl solution in pyridine, Kr^+ laser, 6471-Å line, $P \sim 100$ mW.

surface Raman scattering spectrum of the adsorbed reduction product (see next section).

The nature of wave III (Figure 3) was difficult to analyze in this study. Measurements of scan rate dependencies of the peak current for wave III_c were influenced by the behavior of the nearby wave II_c. Recording of surface Raman data at potentials cathodic of wave III_c proved difficult because of desorption problems. Desorption is expected at these potentials which are cathodic enough to evolve hydrogen. Furthermore, if wave III_c represents a second reduction of the hemin, either of the porphyrin ring or of the central iron to Fe(I),[10] the product would be more negatively charged and would be expected to desorb at these potentials which are cathodic of the potential of zero charge of silver.

Surface Raman Scattering. The surface Raman spectra of adsorbed FePP were obtained with laser excitation wavelengths of 6471, 5145, 4880, 4579, and 4067 Å. Ex situ spectra obtained for the electrodes dipped in either a 0.25 wt % FePPCl/pyridine solution or a 10^{-3} MFePPCl, 0.1 M sodium borate solution, using 6471-Å excitation, are shown in Figure 4. More intense surface Raman spectra of adsorbed FePP were obtained in situ (Figure 5c) following an anodization cycle comparable to that employed by Jeanmaire and van Duyne[11] to observe surface-enhanced Raman scattering from pyridine on silver electrodes. This anodization cycle typically consisted of (1) an anodic step in electrode potential to 0.25 V, (2) development of a charge of 20 mC/cm^2 of electrode area, and (3) a cathodic sweep to −0.1 V to redeposit fresh silver. In general, nearly complete charge reversal occurred in the cathodic sweep to −0.1 V. Anodization of silver at 0.25 V (formation of AgCl) proved more effective in increasing the surface Raman signal than anodization at 0.4 V where soluble silver borates were generated. The anodization at 0.25 V could be accomplished either with the chloride which dissociates from the hemin dissolved in base or, for very dilute solutions of hemin, with added KCl.

Figure 5 illustrates the intensity changes observed in the surface Raman spectrum through the course of the anodization cycle. The

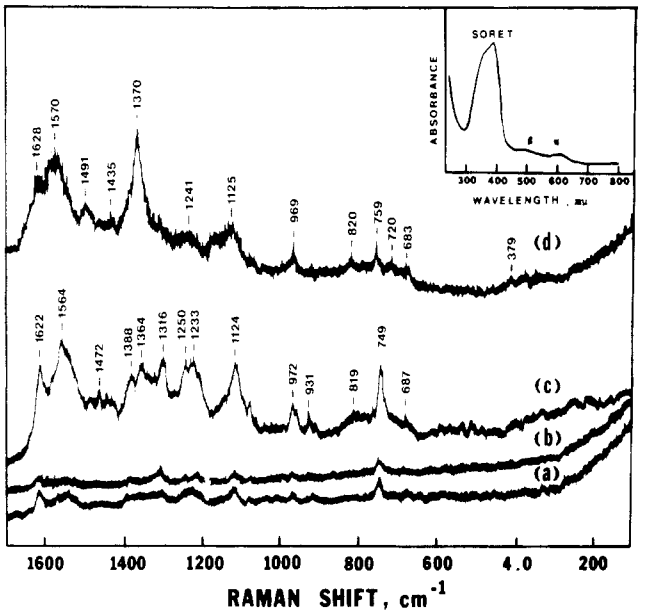

Figure 5. In situ laser Raman spectra of FePPCl on Ag: (a) E = open circuit (OCV) = 0.114 V; (b) E = 0.25 V; (c) E = −0.1 V; (d) E = −0.1 V (Ar^+ laser, 4579-Å line); Kr^+ laser, 6471-Å line for a, b, c; 0.1 M $Na_2B_4O_7$, 4×10^{-6} M FePPCl solution, He saturated. Insert: Absorption spectrum of FePPCl solution in 0.1 M $Na_2B_4O_7$.

lowermost spectrum was recorded at the open circuit voltage (0.144 V) prior to anodization (point A, Figure 1). This spectrum is basically the same as that observed ex situ (Figure 4). The next spectrum (moving up in Figure 5) was recorded at the point of zero current (point B, Figure 1) during the cathodic scan i.e., following anodization and passage of 20 mC/cm^2 charge density but prior to the redeposition of silver metal. The spectrum shows slightly lower intensity than that observed at open circuit but the two spectra are otherwise identical. The spectrum recorded at −0.1 V following the redeposition of silver exhibits a marked increase in intensity compared to the previous one. This spectrum signals the onset of surface Raman intensity enhancement. While the mechanism for enhancement remains controversial, it is generally accepted that enhancement results from a combination of roughness induced modulation of metal electronic resonances and a metal–adsorbate charge-transfer resonance Raman mechanism.[12]

For absorbing adsorbates van Duyne[13] has proposed that both surface Raman enhancement and resonance Raman scattering contribute to the total surface Raman spectrum. Many researchers[14] have observed maximum enhancement with excitation in the red. The lower three spectra in Figure 5 were recorded with 6471-Å excitation. Reference to the UV–visible absorption spectrum of FePP in 0.1 M (insert, Figure 5) indicates that the 6471-Å excitation wavelength is in resonance or preresonance with the porphyrin α band. Thus, the surface Raman spectrum excited with 6471-Å radiation is probably a convolution of α band resonance Raman and surface Raman enhancement.

The spectrum of adsorbed FePP at −0.1 V was also taken with 4579-Å excitation and is reported in Figure 5d. The 4579-Å line will be in resonance with the Soret and β bands. In general, excitation into the Soret band, a dipole allowed transition, provides a resonance Raman spectrum dominated by polarized modes coupled via a Franck–Condon scattering tensor.[15] Excitation in

(10) Brault, D.; Santus, R.; Land, E. J.; Swallow, A. J. *J. Phys. Chem.* **1984**, *88*, 5836.

(11) Jeanmaire, D. L.; van Duyne, R. P. *J. Electroanal. Chem.* **1977**, *84*, 1.

(12) Chang, R. K.; Furtak, T. E., Eds. "Surface Enhanced Raman Scattering"; Plenum: New York, 1982.

(13) Van Duyne, R. P. In "Chemical and Biochemical Applications of Lasers"; Moore, C. B., Ed.; Academic: New York, 1978; Vol. 4.

(14) Creighton, J. A.; Albrecht, M. G.; Hester, R. E.; Matthew, J. A. D. *Chem. Phys. Lett.* **1978**, *55*, 55. Pettinger, B.; Wenning, U.; Kolb, D. M. *Ber. Bunsenges. Phys. Chem.* **1978**, *82*, 1326. Blatchford, C. G.; Campbell, J. R.; Creighton, J. A. *Surf. Sci.* **1981**, *108*, 411. Girlando, A.; Gordon, J. G.; Heitmann, H. D.; Philpott, M. R.; Seki, H.; Swalen, J. D. *Surf. Sci.* **1980**, *101*, 417.

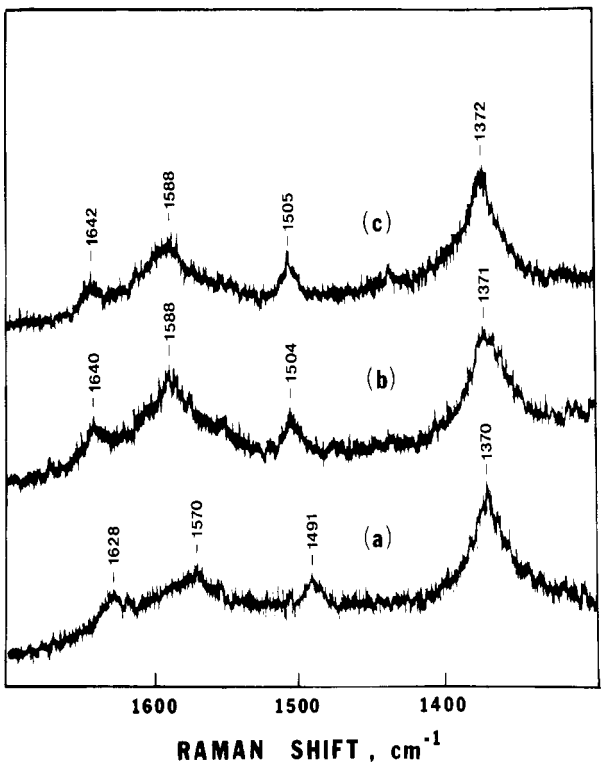

Figure 6. Potential dependence of surface Raman spectra of FePPCl on Ag: (a) $E = -0.1$ V; (b) $E = -0.6$ V; (c) $E = -0.85$ V; 0.1 M $Na_2B_4O_7$, 2×10^{-5} M FePPCl solution; Ar^+ laser, 4579-Å line, $P = 50$–100 mW.

the α (or β) bands, however, is expected to yield a Raman spectrum containing only depolarized or anomalously polarized modes.[16] Unfortunately, all vibrational modes of surface-bound absorbers appear depolarized.[13] For example, the spectrum excited with 4579 Å (Figure 6d) exhibits an intense line at 1370 cm^{-1}. This line corresponds well with the oxidation state marker band at 1373 cm^{-1} (polarized) in the Raman spectrum of aqueous FePP as reported by Verma and Bernstein.[17] This oxidation-state marker band, while polarized in the spectrum of aqueous FePP, exhibits a depolarization ratio of 0.67 for FePP adsorbed at silver. Nonetheless, owing to the volume of published resonance Raman spectra available, the lines observed in the surface Raman spectrum at least under blue excitation, are readily recognizable.

The 1370-cm^{-1} line along with the 1570-cm^{-1} line (Figure 5d) suggests resonance with an allowed (Soret) and forbidden (β) transition by correlating to the oxidation and structure-sensitive lines at 1373 cm^{-1} (polarized) and 1571 cm^{-1} (anomalously polarized), respectively, reported by Verma and Bernstein.[17] The absence of the 1370-cm^{-1} line in the surface Raman spectrum of FePP excited with 6471-Å radiation confirms the lack of Soret band resonance at this excitation wavelength. Therefore, these data imply that the electronic-state distribution in the adsorbed heme is little perturbed from that in solution. The absence of a large perturbation may mean an edge-on adsorption through the carboxylate functionalities. Since the carboxylates do not seem to be involved in coupling the molecular ground and excited states, as evidenced by their absence from the resonance Raman spectrum, binding at these likely sites would not be expected to greatly perturb the porphyrin electronic states. Adsorption of the porphyrin plane parallel to the surface via overlap of electron density of the pyrrole rings would likely involve significant perturbation of the electronic-state energies.

The electrode potential dependence of the surface Raman spectrum of FePP is shown in Figure 6. The spectrum observed at −0.1 V reveals, as before, the oxidation-state marker at 1370 cm^{-1} and the structure-sensitive lines at 1491, 1570, and 1628 cm^{-1}.[17,18] The spectrum observed at −0.6 V, however, shows that all of these lines have been replaced by lines at the higher frequencies of 1371, 1504, 1588, and 1640 cm^{-1}. This spectrum then persists with little further change to the final voltage of our study −0.85 V.

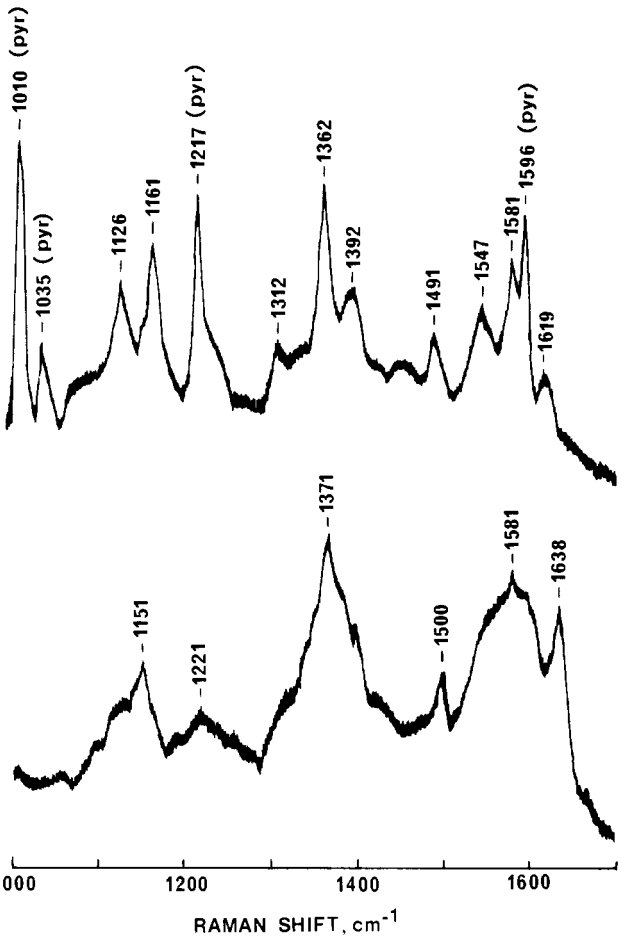

Figure 7. Surface Raman spectra for adsorbed FePP excitation wavelength 5145 Å. Solution: 10 μM FePP in 0.1 M sodium borate, 0.1 M KCl. Applied potential −0.6 V. Bottom: Prior to addition of pyridine to solution. Top: After addition of pyridine to solution.

The shifts to higher frequency exactly parallel that which accompanies a change from high-spin 5-coordinate Fe(III) to intermediate-spin Fe(II) as observed by Spiro and Burke.[19] Spiro reports lines at 1373, 1506, 1589, and 1642 cm^{-1} for intermediate-spin Fe(II)MP which was prepared by reduction of Fe(III)MP with dithionite in a solution devoid of ligands. In that study Spiro confirmed the presence of an Fe(II) product by addition of pyridine and subsequent observation of the resonance Raman spectrum characteristic of 6-coordinate, low-spin $Fe(II)MP(py)_2$. We similarly verified the presence of an Fe(II) reduction product by addition of pyridine to the supporting electrolyte with the potential held at −0.6 V. The surface Raman spectra observed before and after addition of pyridine at −0.6 V are shown in Figure 7. The shift of the oxidation-state marker band from 1371 down to 1362 cm^{-1} upon addition of pyridine along with shifts of the structure-sensitive lines to 1491, 1547, and 1616 cm^{-1} readily flag the presence of a low-spin Fe(II) surface Raman scatterer. Interestingly, several pyridine modes also are observable in the surface Raman spectrum at 1010, 1035, 1217, and 1596 cm^{-1}.[11]

We examined more closely the potential dependence of the surface Raman scattering spectrum for adsorbed FePP in order to locate the potential at which adsorbed Fe(III)PP reduces to

(15) Rousseau, D. L.; Friedmann, J. M.; Williams, P. F. In "Topics in Current Physics"; Weber, A., Ed.; Springer: West Berlin, 1978; Vol 2.
(16) Strekas, T. C.; Spiro, T. G. *J. Raman Spectrosc.* **1973**, *1*, 197.
(17) Verma, A. L.; Bernstein, H. J. *J. Raman Spectrosc.* **1974**, *2*, 163.
(18) Spaulding, L. D.; Chang, C. C.; Yu, N.-T.; Felton, R. H. *J. Am. Chem. Soc.* **1975**, *97*, 2517.
(19) Spiro, T. G.; Burke, J. M. *J. Am. Chem. Soc.* **1976**, *98*, 5482.

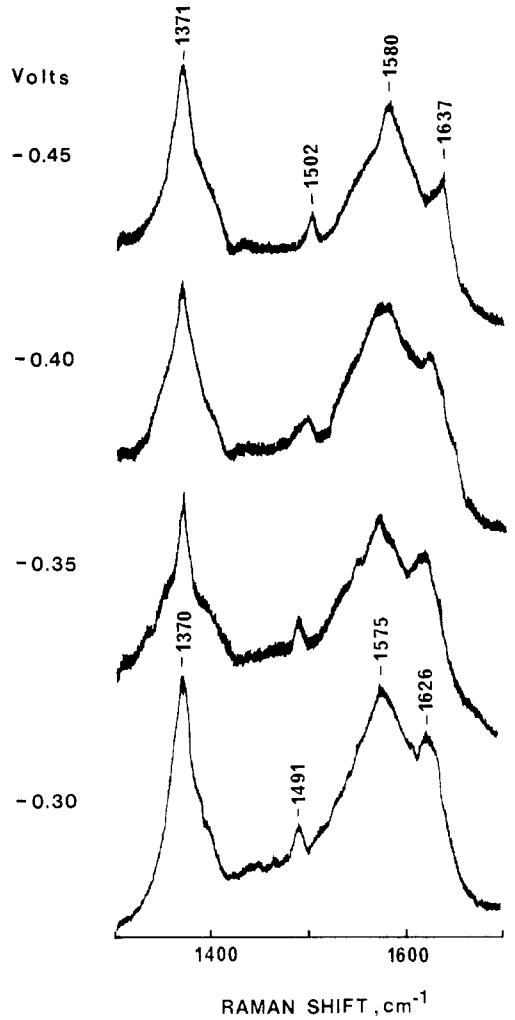

Figure 8. Potential dependence of the surface Raman spectrum for adsorbed hemin in the potential range −0.30 to −0.45 V. Excitation wavelength 4880 Å. Solution concentration of hemin is 15 μM.

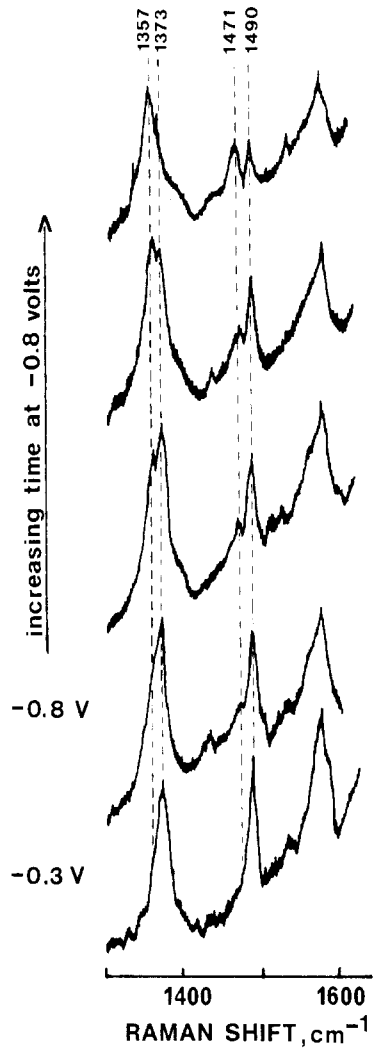

Figure 9. Resonance Raman spectrum of 150 μM FePP in 0.1 M KCl and dilute NaOH (pH 10.5) at −0.3 and −0.8 V. Spectra were obtained by reflecting the laser off of an unanodized electrode. Excitation wavelength 4067 Å.

adsorbed Fe(II)PP. Figure 8 shows the potential dependence of the FePP surface Raman spectrum in a narrow potential range (−0.30 to −0.45 V). At −0.30 V and even at −0.35 V the surface Raman spectrum indicates the continued presence of the oxidized heme as again best characterized by the structure-sensitive lines at 1491, 1575, and 1626 cm^{-1}. At −0.4 V, however, equilibrium between the oxidized and reduced hemin is evidenced in the surface Raman spectrum. Finally, at −0.45 V the reduction appears complete with the structure-sensitive lines at 1502, 1580, and 1637 cm^{-1} clearly identifying the dominant presence of the reduction product. The narrow range over which the adsorbed FePP completely reduces establishes its Nernstian behavior. The spectroscopically determined equilibrium potential near −0.4 V for the surface-bound Fe(III)/Fe(II) redox pair correlated well with the potential of the prewave I_c observed electrochemically (Figure 3) yet lies more than 100 mV anodic of the equilibrium potential for the main wave (wave II_c, Figure 3). Our surface Raman potential dependence, therefore, corroborates the electrochemical designation of wave I_c by Davis and Martin[7] as the reduction of surface-bound FePP. We find even more interesting the fact that the surface Raman scattering is dominated by adsorbates whose potential dependence tracks wave I_c instead of wave II_c. Wave II_c has been electrochemically determined to be associated with reduction of weakly bound hemin. As evidenced in Figure 3, sites of weakly bound hemin represent the overwhelming majority of available sites as estimated from the relative integrated areas of wave I_c and II_c. The strongly bound, perhaps chemisorbed, hemin, though occupying only a small percentage of the available surface sites, is, however, responsible for the observed surface Raman spectrum. These observations match expectations for a chemical enhancement mechanism and further the concept of special sites, e.g., adatoms.[20]

In a recent report by Sanchez and Spiro,[21] the reduction product for adsorbed FePP was identified as a high-spin 5- or 6-coordinate Fe(II). This conclusion was suggested from the observation of a Raman spectrum characteristic of high-spin Fe(II) at very cathodic potentials (−0.8 and −1.0 V). However, their potential-dependent Raman spectra were obtained with 4067-Å excitation which lies strongly in resonance with the Soret absorption (see insert, Figure 6). Resonance Raman scattering from the reduced solution may account for the observed scattering at this excitation wavelength. In order to clarify the source of the dominant scatterer under 4067-Å excitation we repeated the experiment of Sanchez and Spiro with modifications. We examined the Raman spectrum of a solution of 150 μM FePPCl in 0.1 M KCl and dilute base (pH 10.5) in our electrochemical cell by reflecting our laser off an unanodized electrode. At −0.3 V we observed a Raman spectrum (Figure 9) devoid of the small shifts characteristic of the surface-bound hemin. For example, the oxidation-state marker was observed at 1373 cm^{-1}, differing from the surface spectrum reported above for the relatively off resonance lines (4579, 4880, and 5145 Å) i.e., 1371 cm^{-1}, but matching exactly the resonance Raman spectrum reported by Verma and Bernstein.[17] At −0.45 V where adsorbed FePP was observed to be completely reduced (above) no change in the spectrum under 4067-Å excitation was observed even after long times. At −0.8 V, however, changes in the spectrum began to

(20) Otto, A. *J. Electron Spectrosc. Relat. Phenom.* **1983**, *29*, 329.
(21) Sanchez, L. A.; Spiro, T. G. *J. Phys. Chem.* **1985**, *89*, 763.

appear which matched those observed by Sanchez and Spiro. Figure 9 shows the time development of the observed Raman spectrum at −0.8 V which at long times became the spectrum of high-spin Fe(II). The time development of the spectroscopic changes at −0.8 V contrasts the instantaneous changes observed in the reduction of adsorbed hemin and instead tracks the slow reduction of the entire solution volume.

Therefore, it is clear that the reduction product of dissolved hemin and adsorbed hemin have different structures. Our surface Raman data support an intermediate-spin 4-coordinate adsorbed Fe(II)PP and the resonance Raman spectrum of the reduced solution indicates a high-spin more highly coordinated Fe(II)PP structure. The electrochemical data suggest that at high Fe(II) concentrations Fe(II)PP dimers form in solution (see discussion of wave II_a, Figure 3). In the absence of other ligands, the dimerization of dissolved Fe(II)PP may also explain the observation of low-spin Fe(II) in the resonance Raman spectrum of the reduced solution. Apparently, the surface-bound reduction products are restrained from aggregating.

Acknowledgment. J.M. and S.B. thank the Division of Educational Programs, ANL, for support under its Faculty Research Leave and Student Research Participation Programs, respectively. J.M. also acknowledges support by the Herman Goldmann Foundation. We thank Dr. S. Xu for help in obtaining the standard FePPCl spectra ex situ. We thank Professor Gerald T. Babcock of the Department of Chemistry, Michigan State University, for the use of his facility which allowed us to undertake measurement with laser excitation at 4067 Å. This work was supported by the U.S. Department of Energy, Division of Basic Energy Sciences, under Contract W-31-109-Eng-38.

Registry No. FePPCl, 16009-13-5; FePP, 14875-96-8; Ag, 7440-22-4; O_2, 7782-44-7; $Na_2B_4O_7$, 1330-43-4; KCl, 7447-40-7; NaOH, 1310-73-2; pyridine, 110-86-1.

Zero-Field Nuclear Magnetic Resonance of a Nematic Liquid Crystal

A. M. Thayer, J. M. Millar, M. Luzar,† T. P. Jarvie, and A. Pines*

Department of Chemistry, University of California, Berkeley, and Materials and Molecular Research Division, Lawrence Berkeley Laboratory, Berkeley, California 94720 *(Received: October 14, 1985)*

The molecular order parameter of CH_2Cl_2 in a nematic liquid crystal was measured by using a version of zero-field NMR employing pulsed dc magnetic fields. Spectral frequencies and intensities are shown to reflect the ordering on a molecular and macroscopic scale, respectively. Samples oriented in high magnetic field did not significantly change their state of alignment during the time scale of the field cycle. Zero-field measurements of the order parameter yielded values within experimental error of those measured in high field. A zero-field echo experiment was performed to decrease the effect of residual fields on line width. Dipolar order was created in zero field by using a pulsed dc field analogue of the Jeener–Brokaert experiment.

Introduction

Nematic liquid crystals consist of long rodlike molecules whose average orientation is described by a director $\vec{n}$. In the absence of a magnetic field the average orientation of the director is determined by convection and interactions with walls and surfaces of the container of the sample.[1] In a macroscopic sample, $\vec{n}$ is a function of position throughout the sample owing to these effects. Since these materials have an anisotropic magnetic susceptibility defined by $\Delta\chi = \chi_{\parallel} - \chi_{\perp}$, they can be aligned by an applied magnetic field. Given a sample with positive $\Delta\chi$ in an applied field of sufficient magnitude, the system will be describable by a single director whose average alignment is along the field. Molecules of the liquid crystal will on the average be aligned with their long axes parallel to the director.

The magnetic field strength dependence of the alignment on a macroscopic scale has been studied by light scattering,[2] optical[3] and magnetic[4] birefringence, and magnetic susceptibility[5] measurements. The unique feature of NMR is that it measures the alignment on a molecular scale. It has been suggested that the degree of ordering may differ on a macroscopic and molecular level in spite of the small energies of the order director fluctuations.[6] The order parameter and fluctuations are important in relaxation of liquid crystal systems,[7] and it is thus instructive to directly measure the order parameter of a probe molecule in a nematic liquid crystal in high and low fields. The recent pulsed field cycling technique[8-10] of zero-field NMR is ideally suited to this purpose. This paper presents the first applications of zero-field NMR to liquid crystals. A common approach to spectral simplification is to study the behavior of a solute dissolved in the liquid crystal[11,12] since the nematic phase causes the solute to acquire a preferred alignment with respect to the director.[11-13] The allowed motions of the solute reflect the anisotropic molecular tumbling in the uniaxial medium by characteristically averaging the dipolar interaction.[14]

Experimental Section

The system chosen for study was composed of CH_2Cl_2 dissolved in *p*-pentylphenyl 2-chloro-4-(*p*-pentylbenzoyloxy)benzoate (Eastman 11650). Samples were made homogeneous by thoroughly mixing after heating the liquid crystal/solute mixture to above its clearing point. The samples exhibited clearing points

† On leave from Department of Physics and J. Stefan Institute, E. Kardelj University of Ljubljana, Yugoslavia.

(1) G. Meier, E. Sackman, and J. G. Grabmaier, "Applications of Liquid Crystals", Springer-Verlag, West Berlin, 1975.
(2) I. Haller and J. D. Litster, *Phys. Rev. Lett.*, **25**, 1550 (1970); I. Haller and J. D. Litster, *Mol. Cryst. Liq. Cryst.*, **12**, 277 (1977).
(3) E. G. Hanson and Y. R. Shen, *Mol. Cryst. Liq. Cryst.*, **36**, 193 (1976); W. H. de Jeu and P. Bordewijk, *J. Chem. Phys.*, **68**, 109 (1978).
(4) T. W. Stinson and J. D. Litster, *Phys. Rev. Lett.*, **25**, 503 (1970).
(5) J. C. Powell, W. D. Phillips, L. R. Melby, and M. Panar, *J. Chem. Phys.*, **43**, 3442 (1965); H. Gasparoux, B. Regaya, and J. Prost, *C. R. Seances Acad. Sci., Ser. B*, **272**, 1168 (1971).
(6) M. Warner, *Mol. Phys.*, **52**, 677 (1984).
(7) P. R. Luyten, J. Bulthuis, W. M. M. J. Bovee, and L. Plomp, *J. Chem. Phys.*, **78**, 1712 (1983).
(8) J. M. Millar, A. M. Thayer, A. Bielecki, D. B. Zax, and A. Pines, *J. Chem. Phys.*, **83**, 934 (1985).
(9) D. B. Zax, A. Bielecki, K. W. Zilm, A. Pines, and D. P. Weitekamp, *J. Chem. Phys.*, **83**, 4877 (1985).
(10) R. Kreis, D. Suter, and R. R. Ernst, *Chem. Phys. Lett.*, **118**, 120 (1985).
(11) P. Diehl and C. L. Khetrapal, *NMR: Basic Princ. Prog.*, **1** (1969); C. L. Khetrapal, A. C. Kunwar, A. S. Tracey, and P. Diehl, *NMR: Basic Princ. Prog.*, **9** (1975).
(12) J. G. Snijder, C. A. de Lange, and E. E. Burnell, *Isr. J. Chem.*, **23**, 269 (1983).
(13) A. Saupe and G. Englert, *Phys. Rev. Lett.*, **11**, 462 (1963).
(14) P. G. de Gennes, "The Physics of Liquid Crystals", Clarendon Press, Oxford, 1974.

0022-3654/86/2090-1577$01.50/0